9

A Way to Search for Multiferroic Materials with "Unlikely" Combinations of Physical Properties

R.D. James and Z. Zhang

9.1 Introduction

The ideas presented in this chapter begin with the observation by physicists (Hill [1, 2] and Hill and Rabe [3]), probing new phenomena through the use of first principles studies, that the simultaneous occurrence of ferromagnetism and ferroelectricity is unlikely. While these studies do not usually consider the possibility of a phase transformation, there is a lot of indirect evidence that, if the lattice parameters are allowed to change a little, then one might have coexistence of "incompatible properties" like ferromagnetism and ferroelectricity. Thus, one could try the following: seek a reversible first-order phase transformation, necessarily also involving a distortion, from, say, ferroelectric to ferromagnetic phases. If it were highly reversible, there would be the interesting possibility of controlling the volume fraction of phases with fields or stress. The key point is reversibility.

This chapter is an exploration of these ideas. To use these ideas as the basis for the search for new materials there are two major questions that need to be addressed:

1. Why are electromagnetic properties of crystalline materials so sensitive to the precise values of the lattice parameters of the crystal, and how does one understand the dependence?
2. What governs the reversibility of phase transformations?

Here we offer a few thoughts on (1) and a deeper analysis of (2).

Even big first-order phase changes can be highly reversible (liquid water to ice, some shape memory materials), and we argue here that in solids it is the nature of the shape change that is critical. We suggest, based on a close examination of measured hysteresis loops in various martensitic systems, that an idea based on "good fitting of the phases" governs reversibility, and we quantify this idea. The idea lends itself to alloy development and we present work in this direction.

9.2 Single Phase Multiferroics

A prototype for this idea is the search for materials that are both ferromagnetic and ferroelectric. All previous work on the search for materials that are simultaneously ferroelectric and ferromagnetic has been done on single phase materials, or on dual phase materials in which the phases are fixed and may only interact through elasticity. Recently there has been renewed interest in the physics community with the development of methods of density functional theory (DFT) that treat spin accurately. This work is nicely summarized by Hill [1, 2]. The materials that have been discovered, either experimentally or from DFT studies, are mostly of the family $BiXO_3$, the example $BiMnO_3$ having apparently been discovered by DFT. Hill [2] explains why single phase ferroelectric plus ferromagnetic materials are so rare. Briefly, the ferromagnetism is commonly associated with filled $3d$ orbitals, while ferroelectricity, at least in perovskites, is nearly always caused by displacement of the cation which is favored by vacant d orbitals. $BiMnO_3$ just happens to have the "accident" of strongly directional d orbitals that are vacant in just the right directions to promote a ferroelectric displacement. Hill concludes, "Therefore, we should in fact *never* expect the coexistence of ferroelectricity and ferromagnetism."

These studies leave open the possibility of simultaneous ferroelectricity and ferromagnetism in nonperovskite crystal structures. A natural starting place for such studies would be rare earth materials, that utilize unpaired $4f$ electrons. But ferroelectricity is rare in these systems.

Turning these ideas around, if one simply alloys a ferromagnetic oxide with a ferroelectric oxide[1] then one should expect a phase transition. Of course, the phase transformation could be diffusional, and there might be a substantial degradation of e.g., the ferromagnetic properties, as the ferroelectric compound is added.

9.3 Basic Idea

In a nutshell, our idea is that materials with properties that are considered "unlikely" or "impossible" in single phase may become possible in multiphase materials. This is particularly true for certain unlikely combinations of interesting electromagnetic properties. In recent years, based on first principles studies referenced earlier, it has become clear that electromagnetic properties like ferromagnetism, ferroelectricity, and linear (dielectric tensor) and nonlinear optical properties are extremely sensitive to the precise values of the lattice parameters of the material. In a first-order phase transformation involving *a change of lattice parameters* – and therefore a local change of shape – there is

[1]There was substantial empirical work of this type in the former Soviet Union in the late 1950s and early 1960s, also unpublished work from Phillips Lab, involving the replacement of the cation of ferroelectric perovskites by magnetic cations.

the possibility of coexistent phases with completely different properties. If the phase transition is highly reversible, the relative volume fraction of the two phases can be readily changed.

To exhibit this behavior, a material must simultaneously satisfy several conditions (1) the system must have a phase boundary between two distinct phases; (2) it must be possible to induce a transformation from one phase to another by a reasonable applied field or stresses; (3) the kinetics of transformation should be sufficiently fast (i.e., diffusional processes and reordering should be avoided); and (4) the transformation must be highly reversible. Items (2) and (3) suggest the use of martensitic phase transformations which are diffusionless and which also, because of the distortion, can take advantage of the lattice parameter sensitivity of properties. We discuss item (4) in detail later.

9.4 Lattice Parameter Sensitivity

An important piece of insight gained from the first principles' calculations is that the conditions for simultaneous ferromagnetism and ferroelectricity are often highly dependent on the lattice parameters of the material: change the lattice parameters a little and the existence of ferroelectricity/ferromagnetism can change drastically. The issue is well known in the first principles study of ferroelectrics: as Cohen explains in a recent review [4], "Properties of ferroelectrics are extremely sensitive to volume (pressure), which can cause problems since small errors in volume... can result in large errors in computed ferroelectric properties." In fact, it is not that uncommon for workers to adjust lattice parameters to unphysical or nonequilibrium values so as to get ferroelectric properties right.

This sensitivity is also well known in ferromagnetic materials. The oft stated "reason" for ferromagnetism in Heusler alloys like Ni_2MnGa is that the Heusler structure "expands the lattice" by putting the Mn atoms far apart. Similarly, the magnetic properties of strong magnets are improved by diffusing nitrogen into the lattice [5]. The latter is thought not to be due to important band structure interactions involving N but to a small average expansion of the lattice parameter. More recent examples show that this expansion can be affected in $BiFeO_3$ by using epitaxial lattice mismatch to expand the lattice; this has led [6] to the single phase ferroelectric/ferromagnetic with apparently the strongest single-phase polarization/magnetization.

A specific example that does involve a martensitic phase transformation is the ferromagnetic shape memory alloy Ni_2MnGa. This alloy undergoes a diffusionless cubic to tetragonal transformation at $-10°C$ (composition $Ni_{51.3}Mn_{24.0}Ga_{24.7}$) with less than 3°C hysteresis, and having a distortion matrix

$$\mathbf{U}_1 = \begin{pmatrix} 0.952 & 0 & 0 \\ 0 & 1.013 & 0 \\ 0 & 0 & 1.013 \end{pmatrix}, \tag{9.1}$$

i.e., $\mathbf{U}_1$ represents the linear transformation (in the cubic basis) that maps the austenite lattice to the martensite lattice. In transforming from austenite to martensite the saturation magnetization increases about 25%, and the magnetic anisotropy undergoes a dramatic change: austenite is almost perfectly isotropic and saturates at about 600 Oe, while martensite saturates at about 1,000 Oe on the (easy) c-axis and at 12,000 Oe on the (hard) a-axis [7].

What are the origins of this sensitivity to changes of lattice parameters? In general terms sensitivity can arise from various sources, e.g., large mismatch in dimensionless material constants, percolation. In the present case our feeling is that it arises from bifurcation. That is, it seems that the appearance of properties like ferroelectricity and ferromagnetism can be viewed as bifurcations, in which the bifurcation parameters are the lattice parameters. If such bifurcations are of the usual "pitchfork" type, then the implied infinite slope of the bifurcation curve at the bifurcation point implies sensitivity to changes of lattice parameters. Very often, in areas ranging from the structural mechanics of shells to the Jahn–Teller effect [8], bifurcation is associated with broken symmetry. Fortunately, bifurcation theory (with symmetry) can be quantitative, and it is expected that such analyses could guide the implementation of the present idea.

9.5 What Makes Big First Order Phase Transformations Reversible?

For the discussion of the reversibility of martensitic phase transformations we will use the sizes of hysteresis loops as a measure of reversibility. This provides one measure of reversibility, but other measures are also important, e.g., the number of times one can go back and forth through the transformation without unacceptable damage to the material measured via degradation of some physical property. In plasticity, the area inside the initial hysteresis loop correlates in many cases with fatigue life and the simplest theories of plasticity take the "cold work" as proportional to this area. Similar ideas are believed to hold for transformations and the little available data supports this [9]. We will concentrate on shape memory alloys, which already show good reversibility.

The most widely accepted explanations of hysteresis in structural phase transformations arise from two sources (a) pinning of interfaces by defects and (b) thermal activation. A close examination of the experimental data does not, however, seem to support either of these ideas.

Consider, for example, the revealing measurements of hysteresis of Otsuka, Sakamoto, and Shimizu [10] on Cu–14.0Al–4.2Ni (mass%). This alloy is interesting in that it has fully reversible transformations cubic $\rightarrow$ orthorhombic ($\beta_1 \rightarrow \gamma_1'$), cubic $\rightarrow$ monoclinic ($\beta_1 \rightarrow \beta_1'$, $\beta_1 \rightarrow \beta_1''$), as well as intermartensite transitions, also including an α_1' phase. These are all considered highly reversible, but there are dramatic differences in the sizes of the hysteresis

loops. In particular, the $\beta_1 \rightarrow \beta_1'$ transformation has incredibly small hysteresis relative to the others. But this data of Otsuka et al. were all measured *on the same specimen*. Thus, each of these transformations sees the same sea of underlying defects in the material. If "pinning" was the explanation for these dramatic differences in the size of the hysteresis, then it would somehow have to involve the *interaction* of the phase transformation with the defect. But if one looks at all the fundamental measured transformation data for $\beta_1 \rightarrow \beta_1'$ vs. say $\beta_1 \rightarrow \gamma_1'$, e.g., transformation strain, latent heat, elastic moduli of phases, one does not see major differences. In fact, $\beta_1 \rightarrow \beta_1'$ has a bigger transformation strain matrix by any reasonable measure than $\beta_1 \rightarrow \gamma_1'$.

Thermal activation (e.g., transition state theory) also does not seem to be relevant. In fact, the data of Otsuka et al. [10] shows that the hysteresis for the $\beta_1 \rightarrow \beta_1'$ is bigger at higher temperatures, in contradiction to the predictions of theories based on thermal activation.

In the CuZnAl system there are very similar observations, even though the parent phase here has essentially DO_3 ordering. A $\beta_1 \rightarrow \beta_1'$ transformation $Cu_{68}Zn_{15}Al_{17}$ has dramatically smaller hysteresis than the other transformations in this system.

It is also instructive to look at the widely studied NiTiCu system. Certain of these alloys are used in orthodontic applications precisely because of their low hysteresis. Alloys of NiTiCu with 10–20 at. % Cu have the lowest known hysteresis in this system. A tabulation of the width of the hysteresis during stress-induced transformation by Miyazaki and Otsuka [11] is summarized in Table 9.1.

We believe that a completely different idea explains, at least qualitatively, these observations. To explain the idea, in Table 9.2 we write the distortion matrices of the very low hysteresis alloys mentioned earlier (these are obtained from the measured lattice parameters of both phases by formulas given in [12]). For the purpose of comparison, those of NiTi and the cubic to orthorhombic $\beta_1 \rightarrow \gamma_1'$ transformation in $Cu_{69}Al_{27.5}Ni_{3.5}$ are also listed.

Notice first that determinants of all of these matrices are close to 1. Since distortion matrices deform unstressed austenite to unstressed martensite, the determinant measures the volume ratio of martensite to austenite,

Table 9.1. Width of the stress hysteresis in NiTiCu alloys according to Miyazaki and Otsuka [11]

Alloy	Width of the hysteresis (MPa)
$Ti_{41.5}Ni_{48.5}Cu_{10.0}$	400
$Ti_{45.5}Ni_{49.5}Cu_{5.0}$	300
$Ti_{44.5}Ni_{50.5}Cu_{5.0}$	200
$Ti_{44.5}Ni_{45.5}Cu_{10.0}$	100
$Ti_{45.5}Ni_{44.5}Cu_{10.0}$	100
$Ti_{50.0}Ni_{40.0}Cu_{10.0}$	100

Table 9.2. Distortion matrices for various transformations with their eigenvalues and determinant

Alloy	Distortion matrix	Eigenvalues	Determinant
$Ni_{50}Ti_{50}$	$\begin{pmatrix} 1.0243 & 0.05803 & -0.04266 \\ 0.05803 & 1.0243 & -0.04266 \\ -0.04266 & -0.04266 & 0.9563 \end{pmatrix}$	1.1066 **0.9663** 0.9321	0.9966
$\mathbf{Ni_{40.5}Ti_{49.5}Cu_{10.0}}$	$\begin{pmatrix} 1.0260 & -0.02740 & 0 \\ -0.02740 & 1.0260 & 0 \\ 0 & 0 & 0.9508 \end{pmatrix}$	1.0534 **0.9986** 0.9508	1.0002
$Cu_{69}Al_{27.5}Ni_{3.5}$ $(\beta_1 \to \gamma_1')$	$\begin{pmatrix} 1.0424 & 0.0194 & 0 \\ 0.0194 & 1.0424 & 0 \\ 0 & 0 & 0.9178 \end{pmatrix}$	1.0618 **1.0230** 0.9178	0.9969
$\mathbf{Cu_{69}Al_{27.5}Ni_{3.5}}$ $(\beta_1 \to \beta_1')$	$\begin{pmatrix} 1.0716 & 0.0516 & 0 \\ 0.0516 & 1.0311 & 0 \\ 0 & 0 & 0.9127 \end{pmatrix}$	1.1067 **0.9959** 0.9127	1.0060
$\mathbf{Cu_{68}Zn_{15}Al_{17}}$ $(\beta_1 \to \beta_1')$	$\begin{pmatrix} 1.087 & 0.0250 & 0 \\ 0.0250 & 1.010 & 0 \\ 0 & 0 & 0.9093 \end{pmatrix}$	1.0944 **1.0026** 0.9093	0.9977

The alloys shown in bold have the lowest hysteresis in their respective systems; middle eigenvalues are also shown in bold

so a determinant of 1 means no volume change. It is well understood that this condition is important for reversibility, especially in polycrystals: if there is a volume change then an island of martensite growing in austenite would generate stress and vice versa. This would happen both ways through the transformation, and therefore any (total) free energy decreasing path between phases would necessarily be part of a hysteretic loop. According to a result of Bhattacharya [13], in a material with cubic austenite, $\det = 1$ is also *sufficient* that there be a microstructure of martensite filling an interior region, with no long range stresses, that satisfies the boundary conditions imposed by the surrounding austenite. However, all the determinants listed in Table 9.2 apparently must be sufficiently close to 1 to minimize this effect on hysteresis, as there does not seem to be a correlation with the low hysteresis cases.[2]

However, there is a striking correlation between the low hysteresis alloys and the condition $\lambda_2 = 1$, where $\lambda_1 \leq \lambda_2 \leq \lambda_3$ are the ordered eigenvalues of the distortion matrix. From Table 9.2 one can see that $|\lambda_2 - 1|$ is an order of magnitude smaller in the low hysteresis alloys than in the others.

[2]Though we should add that these were measurements of hysteresis in stress-induced transformation, and also the measurements on the copper based alloys were done on single crystals. While there is typically a correlation between stress-induced and temperature-induced hysteresis, the full explanation for the relevance of the special conditions could be more subtle.

The condition $\lambda_2 = 1$ is relevant to issues of compatibility [14]. This condition is necessary and sufficient that the austenite be exactly compatible with the martensite (without fine twinning). Mathematically, given a symmetric distortion matrix $\mathbf{U}_1$, the condition $\lambda_2 = 1$ is necessary and sufficient that there exist a rotation matrix $\mathbf{R}$ and a pair of vectors $\mathbf{a}, \mathbf{n}$ such that

$$\mathbf{R}\mathbf{U}_1 - \mathbf{I} = \mathbf{a} \otimes \mathbf{n}. \tag{9.2}$$

In fact, if $\lambda_2 = 1$, there are precisely two solutions $(\mathbf{R}_1, \mathbf{a}_1 \otimes \mathbf{n}_1)$ and $(\mathbf{R}_2, \mathbf{a}_2 \otimes \mathbf{n}_2)$ of (9.2) and these can be written down explicitly [12, 14]. This contrasts sharply with the typical case $\lambda_2 \neq 1$. In that case the typical microstructure at transition is shown in Fig. 9.1.

As is well known in the theory of martensite, the microstructure of Fig. 9.1 is governed by the crystallographic theory of martensite. For our later purposes we will need to describe a few of the results of that theory. First, we need to display the full set distortion matrices corresponding to the martensite. There is a theory for constructing these [15] based on symmetry and the Ericksen–Pitteri neighborhood, but we will just present the final results, shown below in the cases relevant to this chapter.

1. Cubic to tetragonal:

$$\mathbf{U}_1 = \begin{pmatrix} \beta & 0 & 0 \\ 0 & \alpha & 0 \\ 0 & 0 & \alpha \end{pmatrix}, \quad \mathbf{U}_2 = \begin{pmatrix} \alpha & 0 & 0 \\ 0 & \beta & 0 \\ 0 & 0 & \alpha \end{pmatrix}, \quad \mathbf{U}_3 = \begin{pmatrix} \alpha & 0 & 0 \\ 0 & \alpha & 0 \\ 0 & 0 & \beta \end{pmatrix}. \tag{9.3}$$

2. Cubic to orthorhombic:

$$\mathbf{U}_1 = \begin{pmatrix} \alpha & \delta & 0 \\ \delta & \alpha & 0 \\ 0 & 0 & \beta \end{pmatrix}, \quad \mathbf{U}_2 = \begin{pmatrix} \alpha & 0 & \delta \\ 0 & \beta & 0 \\ \delta & 0 & \alpha \end{pmatrix}, \quad \mathbf{U}_3 = \begin{pmatrix} \beta & 0 & 0 \\ 0 & \alpha & \delta \\ 0 & \delta & \alpha \end{pmatrix},$$

$$\mathbf{U}_4 = \begin{pmatrix} \alpha & -\delta & 0 \\ -\delta & \alpha & 0 \\ 0 & 0 & \beta \end{pmatrix}, \quad \mathbf{U}_5 = \begin{pmatrix} \alpha & 0 & -\delta \\ 0 & \beta & 0 \\ -\delta & 0 & \alpha \end{pmatrix}, \quad \mathbf{U}_6 = \begin{pmatrix} \beta & 0 & 0 \\ 0 & \alpha & -\delta \\ 0 & -\delta & \alpha \end{pmatrix}.$$

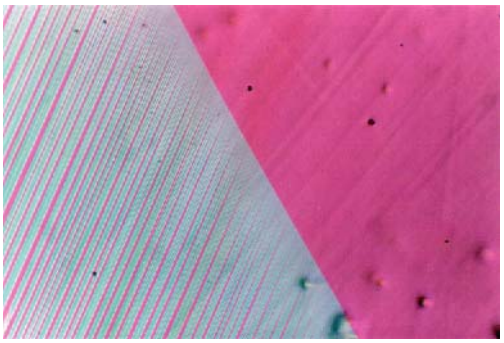

Fig. 9.1. Austenite/martensite interface in the $\beta_1 \to \gamma_1'$ transformation of $Cu_{69}Al_{27.5}Ni_{3.5}$. (Picture courtesy: C. Chu)

3. Cubic to monoclinic
   (a) $\langle 110\rangle$ polarized:

$$\mathbf{U}_1 = \begin{pmatrix} \sigma & \tau & \rho \\ \tau & \sigma & \rho \\ \rho & \rho & \xi \end{pmatrix}, \quad \mathbf{U}_2 = \begin{pmatrix} \sigma & \rho & \tau \\ \rho & \xi & \rho \\ \tau & \rho & \sigma \end{pmatrix}, \quad \mathbf{U}_3 = \begin{pmatrix} \xi & \rho & \rho \\ \rho & \sigma & \tau \\ \rho & \tau & \sigma \end{pmatrix},$$

$$\mathbf{U}_4 = \begin{pmatrix} \sigma & -\tau & -\rho \\ -\tau & \sigma & \rho \\ -\rho & \rho & \xi \end{pmatrix}, \quad \mathbf{U}_5 = \begin{pmatrix} \sigma & -\rho & -\tau \\ -\rho & \xi & \rho \\ -\tau & \rho & \sigma \end{pmatrix}, \quad \mathbf{U}_6 = \begin{pmatrix} \xi & -\rho & -\rho \\ -\rho & \sigma & \tau \\ -\rho & \tau & \sigma \end{pmatrix},$$

$$\mathbf{U}_7 = \begin{pmatrix} \sigma & -\tau & \rho \\ -\tau & \sigma & -\rho \\ \rho & -\rho & \xi \end{pmatrix}, \quad \mathbf{U}_8 = \begin{pmatrix} \sigma & -\rho & \tau \\ -\rho & \xi & -\rho \\ \tau & -\rho & \sigma \end{pmatrix}, \quad \mathbf{U}_9 = \begin{pmatrix} \xi & -\rho & \rho \\ -\rho & \sigma & -\tau \\ \rho & -\tau & \sigma \end{pmatrix},$$

$$\mathbf{U}_{10} = \begin{pmatrix} \sigma & \tau & -\rho \\ \tau & \sigma & -\rho \\ -\rho & -\rho & \xi \end{pmatrix}, \quad \mathbf{U}_{11} = \begin{pmatrix} \sigma & \rho & -\tau \\ \rho & \xi & -\rho \\ -\tau & -\rho & \sigma \end{pmatrix}, \quad \mathbf{U}_{12} = \begin{pmatrix} \xi & \rho & -\rho \\ \rho & \sigma & -\tau \\ -\rho & -\tau & \sigma \end{pmatrix}.$$

   (b) $\langle 100\rangle$ polarized:

$$\mathbf{U}_1 = \begin{pmatrix} \rho & \sigma & 0 \\ \sigma & \tau & 0 \\ 0 & 0 & \beta \end{pmatrix}, \quad \mathbf{U}_2 = \begin{pmatrix} \tau & 0 & \sigma \\ 0 & \beta & 0 \\ \sigma & 0 & \rho \end{pmatrix}, \quad \mathbf{U}_3 = \begin{pmatrix} \beta & 0 & 0 \\ 0 & \rho & \sigma \\ 0 & \sigma & \tau \end{pmatrix},$$

$$\mathbf{U}_4 = \begin{pmatrix} \tau & \sigma & 0 \\ \sigma & \rho & 0 \\ 0 & 0 & \beta \end{pmatrix}, \quad \mathbf{U}_5 = \begin{pmatrix} \rho & 0 & \sigma \\ 0 & \beta & 0 \\ \sigma & 0 & \tau \end{pmatrix}, \quad \mathbf{U}_6 = \begin{pmatrix} \beta & 0 & 0 \\ 0 & \tau & \sigma \\ 0 & \sigma & \rho \end{pmatrix},$$

$$\mathbf{U}_7 = \begin{pmatrix} \rho & -\sigma & 0 \\ -\sigma & \tau & 0 \\ 0 & 0 & \beta \end{pmatrix}, \quad \mathbf{U}_8 = \begin{pmatrix} \tau & 0 & -\sigma \\ 0 & \beta & 0 \\ -\sigma & 0 & \rho \end{pmatrix}, \quad \mathbf{U}_9 = \begin{pmatrix} \beta & 0 & 0 \\ 0 & \rho & -\sigma \\ 0 & -\sigma & \tau \end{pmatrix},$$

$$\mathbf{U}_{10} = \begin{pmatrix} \tau & -\sigma & 0 \\ -\sigma & \rho & 0 \\ 0 & 0 & \beta \end{pmatrix}, \quad \mathbf{U}_{11} = \begin{pmatrix} \rho & 0 & -\sigma \\ 0 & \beta & 0 \\ -\sigma & 0 & \tau \end{pmatrix}, \quad \mathbf{U}_{12} = \begin{pmatrix} \beta & 0 & 0 \\ 0 & \tau & -\sigma \\ 0 & -\sigma & \rho \end{pmatrix}.$$

Note that there are two ways to transform from cubic to monoclinic phases, which we label $\langle 110\rangle$ polarized and $\langle 100\rangle$ polarized. We should also remark that many martensitic transformations involve shuffling. In that case the crystal structures of austenite and martensite can each be viewed as the union of a set of identical interpenetrating Bravais lattices, translated with respect to each other. In that case the meaning of a distortion matrix is a matrix of a linear transformation (again, with respect to the cubic basis) that maps one of these Bravais lattices for austenite to the corresponding one for martensite. This definition is consistent with the measurements presented earlier for particular systems.

To describe the microstructure in Fig. 9.1, we consider two variants of martensite, described by two distortion matrices, say, $\mathbf{U}_1$ and $\mathbf{U}_2$. To describe the bands of martensite on the left of Fig. 9.1, we solve the "twinning equation,"

$$\mathbf{R}\mathbf{U}_2 - \mathbf{U}_1 = \mathbf{a} \otimes \mathbf{n}\,, \tag{9.4}$$

$\mathbf{R}$ being a rotation matrix. As above, we get two solutions $\mathbf{R}^{\mathrm{I}}, \mathbf{a}^{\mathrm{I}}, \mathbf{n}^{\mathrm{I}}$ and $\mathbf{R}^{\mathrm{II}}, \mathbf{a}^{\mathrm{II}}, \mathbf{n}^{\mathrm{II}}$, these being associated with Type I and Type II twins. We call a solution $(\mathbf{a}, \mathbf{n})$ of (9.4) a *twin system*. Taking one of these solutions, one can make a compatible layering of these distortions, $\mathbf{R}\mathbf{U}_2/\mathbf{U}_1/\mathbf{R}\mathbf{U}_2/\mathbf{U}_1$, etc., with a suitable volume fraction λ of say variant 2. This describes the structure on the left of Fig. 9.1. Introducing a transition layer between this layering and the austenite phase, one finds that the elastic energy in this transition layer can be made arbitrarily small by making the twins finer and finer, if and only if the following equation holds,

$$\hat{\mathbf{R}}\,(\lambda \mathbf{R}\mathbf{U}_2 + (1-\lambda)\mathbf{U}_1) = \mathbf{I} + \mathbf{b} \otimes \mathbf{m}\,, \tag{9.5}$$

for some rotation matrix $\hat{\mathbf{R}}$ and vectors $\mathbf{b}, \mathbf{m}$. Here $\mathbf{m}$ is the normal to the austenite/martensite interface, and $\hat{\mathbf{R}}$ is a suitable rigid body rotation of the martensite laminate needed to secure this approximate compatibility. Equations (9.4) and (9.5) comprise one form of the equations of the crystallographic theory of martensite.

Given a twin system, the calculation of the solution of (9.5) is quite rigid in the usual case $\lambda_2 \neq 1$. One finds [14] that given the twin system $(\mathbf{a}, \mathbf{n})$ there are four values of $\mathbf{b} \otimes \mathbf{m}$, that is, four austenite/martensite interfaces, corresponding to just two values[3] of the volume fraction λ. The shape changes, angles between boundaries, and volume fractions predicted by this calculation agree very well with those shown in Fig. 9.1, and with a great many other cases.

The crystallographic theory of martensite does not determine the fineness of microstructure. That is believed to involve a balance between the interfacial energy of the twin boundaries on the left of Fig. 9.1 and the elastic energy in the transition layer. In fact if one looks closely at Fig. 9.1 then one sees that there is branching of the twins near the interface. This is also understood (Kohn and Müller [16]) as a mechanism for reducing energy, in which the elastic energy of the transition layer becomes delocalized and the twins split into finer and finer arrays near the interface, but always with the volume fraction given by (9.5). In any case the energy of the austenite/martensite interface is the sum of bulk and interfacial energies arising from incompatibility of austenite and martensite. This energy has to be created both ways through the transformation. Any free energy decreasing path from one phase to the other must therefore be part of a hysteretic loop.

---

[3] Two interfaces have volume fraction, say, λ^*, and the other two have volume fraction $(1-\lambda^*)$.

However, if $\lambda_2 = 1$, then austenite *is* compatible with martensite and both elastic and interfacial energies are avoided, except for the single (likely atomically sharp) interface separating austenite and martensite. Since many millions of these austenite/martensite interfaces may be created in a macroscopic sample during transformation, one can imagine that $\lambda_2 = 1$ can be relevant for hysteresis, as noticed earlier.

We have discussed two conditions for reversibility: $\det \mathbf{U}_1 = 1$ and $\lambda_2 = 1$, λ_2 being the middle eigenvalue of $\mathbf{U}_1$. Due to the structure of distortion matrices [15], both the middle eigenvalue and the determinant of all distortion matrices corresponding to a given transformation (e.g., as listed earlier) are the same. We now propose to introduce a third set of conditions, we call the *cofactor conditions*, at which an even more spectacular "accident" of compatibility occurs. The cofactor conditions presuppose that $\lambda_2 = 1$, and they also depend on the choice of the twin system, $\mathbf{a}, \mathbf{n}$. These conditions can be easily extracted from the treatment of the crystallographic theory in [14], although one of the hypotheses was inadvertently omitted there. The cofactor conditions are

$$\lambda_2 = 1, \quad \operatorname{tr} \mathbf{U}_1^2 - \det \mathbf{U}_1^2 - 2 - \frac{1}{4}|\mathbf{a}|^2 > 0, \quad \mathbf{a} \cdot \mathbf{U}_1 \operatorname{cof} (\mathbf{U}_1^2 - \mathbf{I})\mathbf{n} = 0\,. \tag{9.6}$$

Here, cof A denotes the cofactor of the matrix A: $(\operatorname{cof} A)_{ij} = (-1)^{i+j} \det \hat{A}_{ij}$, where $\hat{A}$ is the 2×2 matrix obtained by deleting the ith row and jth column of A. If the cofactor conditions are satisfied, then, *in addition to the austenite single-variant interfaces arising from* $\lambda_2 = 1$*, it is possible to have austenite/martensite interfaces with any volume fraction*[4] *between* 0 *and* 1.

As an example, a distortion matrix belonging to a cubic to monoclinic transformation ($\langle 100 \rangle$ polarized) that satisfies exactly the cofactor conditions is

$$\mathbf{U}_1 = \begin{pmatrix} 1.09 & 0.030 & 0 \\ 0.030 & 1.010 & 0 \\ 0 & 0 & 0.93 \end{pmatrix}. \tag{9.7}$$

[Here, the chosen twin system is the Type I twin relating variants 1 and 12, the notation as above, which gives $\mathbf{a} = (-0.17182, -0.0572727, 0.145266)$, $\mathbf{n} = (101)$.] Notice that this matrix is not far away from the real measured transformation matrix of $Cu_{68}Zn_{15}Al_{17}$, Table 9.2. The best way to illustrate the result in italics just above is to plot a family of austenite/martensite interfaces corresponding to a sequence of volume fractions going from 0 to 1. This is done in Fig. 9.2. This should be contrasted with the restrictive results (4 interfaces, just 2 volume fractions) mentioned above in the usual case when the cofactor conditions are not satisfied.

---

[4] If the inequality in (9.6) is weakened to the statement $\operatorname{tr} \mathbf{U}_1^2 - \det \mathbf{U}_1^2 - 2 > 0$, then there is a limited range of volume fractions, given precisely by $[0, \lambda^*] \cup (1 - \lambda^*, 1]$, where $\lambda^* = \frac{1}{2}\left(1 - \sqrt{1 - 4(\mu/|\mathbf{a}|^2)}\right)$ and $\mu = \operatorname{tr} \mathbf{U}_1^2 - \det \mathbf{U}_1^2 - 2$, for which there are austenite/martensite interfaces.

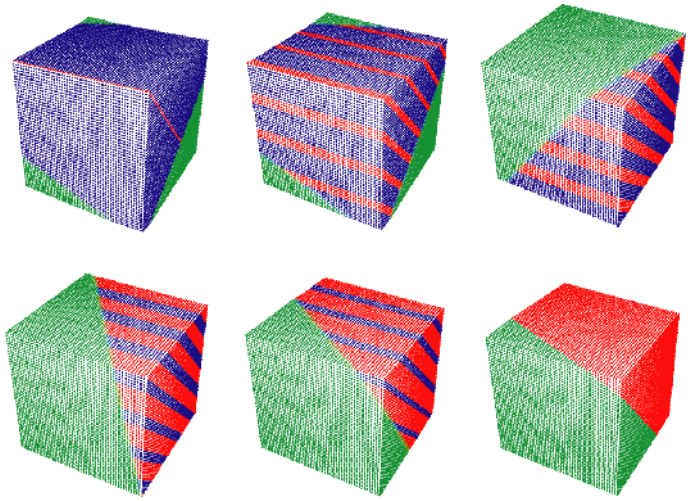

Fig. 9.2. Illustration of the continuous variation of volume fraction of martensite possible under the cofactor conditions. Distortions accurately drawn using the distortion matrix and twin system given in $(9.7)_{\text{ff}}$

Note the remarkable degree of flexibility indicated by these pictures. In fact, as the volume fraction of martensite goes from 0 to 1, the (perpendicular) directions of maximum and minimum principle strain in the martensite actually exchange places. Thus, these special conditions on lattice parameters do not mean that the martensite is compatible with the austenite because it does not deform with volume fraction changes. On the contrary, it undergoes large average deformations *while* remaining compatible with austenite.

One possible objection to the usefulness of the cofactor conditions is that they only appear to apply to one twin system. As we shall see later, this is not the case. In cubic to monoclinic transformations, if the cofactor conditions are satisfied for one twin system, then they are satisfied for many twin systems.

9.6 Specific Relationships Among Lattice Parameters for a High Degree of Reversibility

Here we answer the question of what precisely are the conditions on lattice parameters that imply the satisfaction of the proposed conditions for reversibility. It is easy to write down the conditions $\det \mathbf{U}_1 = 1$ and $\lambda_2 = 1$ in terms of the parameters in $\mathbf{U}_1$, so, instead, we concentrate on the most interesting case of satisfying simultaneously all of the conditions: $\det \mathbf{U}_1 = 1$, $\lambda_2 = 1$ and the cofactor conditions. We focus only on cases where the austenite is cubic, and the symmetries have a group/subgroup relationship. In this case it is easy to see that the full set of conditions cannot be satisfied if the distortion is

such that the martensite has tetragonal or trigonal (rhombohedral), symmetry, but can be satisfied for lower symmetry martensites, as discussed later. Later, when we discuss the variants of martensite, we refer to the numbering of distortion matrices given in Sect. 9.5.

9.6.1 Cubic to Orthorhombic Transformations

In the cubic to orthorhombic case there are precisely two matrices that satisfy all three conditions. These matrices are

$$\mathbf{U}_1^{\mathrm{I}} = \begin{pmatrix} \frac{1}{2}(1+\frac{1}{\sqrt{2}}) & \frac{1}{2}(1-\frac{1}{\sqrt{2}}) & 0 \\ \frac{1}{2}(1-\frac{1}{\sqrt{2}}) & \frac{1}{2}(1+\frac{1}{\sqrt{2}}) & 0 \\ 0 & 0 & \sqrt{2} \end{pmatrix}, \quad \mathbf{U}_1^{\mathrm{II}} = \begin{pmatrix} \frac{1}{2}(1+\sqrt{2}) & \frac{1}{2}(\sqrt{2}-1) & 0 \\ \frac{1}{2}(\sqrt{2}-1) & \frac{1}{2}(1+\sqrt{2}) & 0 \\ 0 & 0 & \frac{1}{\sqrt{2}} \end{pmatrix}.$$

Each of these matrices satisfies the cofactor conditions simultaneously for 12 twin systems, all Type I twins for the case of $\mathbf{U}_1^{\mathrm{I}}$ and all Type II twins for the case of $\mathbf{U}_1^{\mathrm{II}}$ (the compound twins never satisfy all three conditions). These are quite big matrices by any measure, and therefore unlikely to be realistic; they may also fall outside of the Ericksen–Pitteri neighborhood and therefore call into question the basic theory. Nevertheless, they are useful for the purpose of illustration.

9.6.2 Cubic to Monoclinic Transformations

⟨100⟩-Polarized

In the ⟨100⟩ polarized cubic to monoclinic case there are two one-parameter families of matrices satisfying all three conditions, given below.

$$\mathbf{U}_1^{\mathrm{I}} = \begin{pmatrix} \alpha+\alpha^2-\alpha^3 & \sqrt{\alpha^2(1+\alpha)(1-\alpha)^3} & 0 \\ \sqrt{\alpha^2(1+\alpha)(1-\alpha)^3} & 1-\alpha^2+\alpha^3 & 0 \\ 0 & 0 & \frac{1}{\alpha} \end{pmatrix}, \quad \alpha \le 1\,, \quad (9.8)$$

$$\mathbf{U}_1^{\mathrm{II}} = \begin{pmatrix} (\alpha^2+\alpha-1)/\alpha^2 & \frac{1}{\alpha^2}\sqrt{(\alpha-1)^3(\alpha+1)} & 0 \\ \frac{1}{\alpha^2}\sqrt{(\alpha-1)^3(\alpha+1)} & (\alpha^3-\alpha+1)/\alpha^2 & 0 \\ 0 & 0 & \frac{1}{\alpha} \end{pmatrix}, \quad \alpha \ge 1\,. \quad (9.9)$$

Each of these works simultaneously for 12 twin systems. These are Type I twins in case (9.8) and Type II twins in case (9.9), but not all are included (i.e., there are more than 12 Type I twins in this system). Note that both families begin at the identity, corresponding to no transformation, at $\alpha = 1$. The case (9.9) is particularly interesting in its proximity to real examples of distortion matrices.

There are also several one-parameter families corresponding to $\beta = 1$ in the notation above. These are less interesting because they do not seem to be close to any realistic cases that could provide starting points for alloy development. On the other hand, some of these cases apply to many twin systems.

⟨110⟩-Polarized

In the ⟨110⟩ polarized cubic to monoclinic case there are several one-parameter families of matrices satisfying all three conditions. We found seven such families, all passing through the identity, and all applying simultaneously to multiple twin systems. There is also a two-parameter family of matrices satisfying all three conditions, but only applying to a limited family of compound twins. While it is possible to write analytical expressions for the seven families matrices satisfying these conditions, these are somewhat complicated to write down so we do not give them here.

9.6.3 Relationships for Martensite/Martensite Transitions

The conditions we propose for reversibility are applicable to martensite–martensite transitions, such as the tetragonal to trigonal transformation that occurs at a morphotropic boundary. These should imply low hysteresis by the same reasoning that we have given for the austenite/martensite transitions. If $\mathbf{U}$ and $\mathbf{V}$ denote (positive-definite, symmetric) distortion matrices corresponding to two different martensites, the condition (1) of no volume change is $\det \mathbf{U} = \det \mathbf{V}$, (2) the exact compatibility is that the middle eigenvalue of $\mathbf{V}^{-1}\mathbf{U}^2\mathbf{V}^{-1}$ is 1. The cofactor conditions are (9.4) and (9.5) with $\mathbf{U}_1, \mathbf{U}_2$ replaced by $\mathbf{U}, \mathbf{V}$, respectively, and $\mathbf{I}$ replaced by either $\mathbf{U}$ or $\mathbf{V}$. It is also possible to pass from the description (9.4) and (9.5) to more compact conditions like (9.6) in the martensite/martensite case using the methods of [14]. There are also further conditions that would make two compatible laminates of martensite additionally flexible, that would likely also enhance the reversibility of transition.

9.7 Tuning Lattice Parameters to Satisfy Two of the Proposed Conditions in the NiTiCuPd System

We have recently put these ideas into practice in a special case, that of the NiTiCuPd system. It is known that a family of alloys in the system NiTiCu nearly satisfy the second condition $\lambda_2 = 1$, which suggested to us that this is a good starting place. We focused on trying to determine the alloys that satisfy just the first two conditions $\det \mathbf{U}_1 = 1$ and $\lambda_2 = 1$.

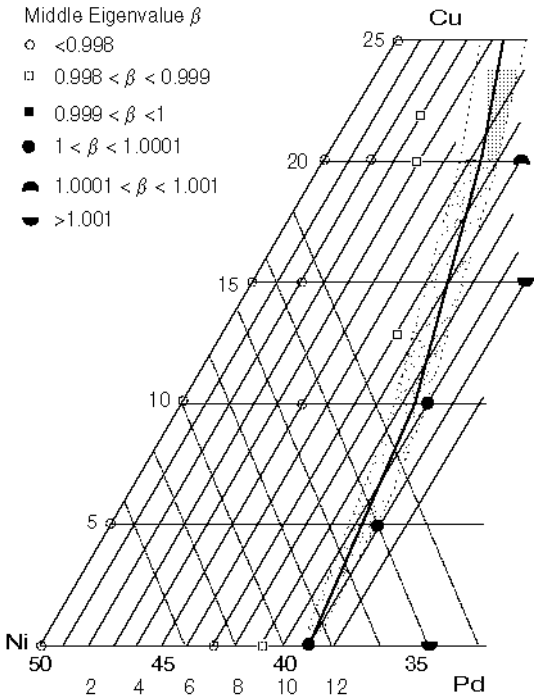

Fig. 9.3. A part of the compositional triangle NiCuPd at Ti = 50%. Compositions on the line satisfy the condition $\lambda_2 = \beta = 1$. A small subset of the measured samples is also shown. The *shaded region* indicates the error expected in this determination

Briefly, we measured lattice parameters of both austenite and martensite by X-ray diffraction and thereby established the mapping between composition and distortion matrices. (For a more detailed description of these experiments, see Zhang [17].)

Over a large compositional region we found that $\det \mathbf{U}_1 = 1$ within our error of measurement. However, the middle eigenvalue λ_2 was more sensitive to composition.[5] An example of our results is shown in Fig. 9.3. The compositional space NiTiCuPd is three-dimensional. Figure 9.3 shows a 2D slice through this surface at constant Ti composition of 50%.

9.8 Further Comparisons with Experiment

After determining the mapping between composition and distortion matrices as described in Sect. 9.7, we were informed of additional data on hysteresis in the literature for alloys of particular composition. (We are grateful to Wuttig, Quandt, and Berg for these references.)

---

[5] Also, the error of the measurement of λ_2 was smaller than that of $\det \mathbf{U}_1$.

We first describe measurements of Winzek and Quandt [18]. They measured thermal hysteresis in both free standing and stressed films, and both had similar trends, but, for definiteness, we compare with the measurements on the free standing films. Winzek and Quandt also measured hysteresis in two different ways: by using the width of a parallelogram approximation of the loop, and by using the thinnest place on the loop (some loops had a "waist"). We compare with the former method. In their measurements on NiTiCu, they found that an alloy with approximate composition $Ni_{34}Ti_{50}Cu_{16}$ exhibited the lowest hysteresis among alloys they studied. We did not find any alloys in the NiTiCu system that satisfy $\lambda_2 = 1$ within our experimental error. However, the alloy in the NiTiCu system that most closely satisfies $\lambda_2 = 1$ is $Ni_{30}Ti_{50}Cu_{20}$, which is quite close to that of Winzek and Quandt (in fact, the closest of those they measured). We believe that if they had measured the alloy $Ni_{30}Ti_{50}Cu_{20}$, it would have exhibited the lowest hysteresis.

More interestingly, Winzek and Quandt [18] also made similar measurements on NiTiPd films. They found that there was a rather sharp drop in the hysteresis at the composition $Ni_{40}Ti_{50}Pd_{10}$, among alloys they tested. This is very close to the crossing point of our surface $\lambda_2 = 1$, as can be seen from Fig. 9.3; in fact, the exact crossing is at $Ni_{39}Ti_{50}Pd_{11}$.

Also interesting is the data we have collected from the US Patent 5, 951, 793 shown in Table 9.3. Some of these alloys have small percentages of elements that we have not studied, and these can either be excluded from the comparison or else included (by, e.g., assigning their percent to the element for which they substitute). It is seen from Table 9.3 that there are dramatic differences in the size of the stress hysteresis. The closest alloy to our surface $\lambda_2 = 1$ is the alloy shown in bold and it is indeed very close. This is the one with the lowest hysteresis.

Table 9.3. Data on stress hysteresis vs. composition for various alloys collected from US Patent 5,951,793

Ti	Ni	Pd	Other	Width of the hysteresis (MPa)	A_f (°C)
49.5	43.5	0	Cu 7	236	25
50	40	0	Cu 10	172	60
50	47	2.5		263	55
49.5	47	3	Cr 0.5	148	5
49.5	46.5	4		137	5
50	42.5	7.5		95	25
50	42	7.5	Co 0.5	82	15
49.5	**40.5**	**10**		**54**	**−20**
49.5	38	12	V 0.5	106	30
49	36	13	Fe 2	103	−30
51	35	14		127	60
49	36	15		170	−50

9.9 Summary and Outlook: A General Method for Seeking New Classes of Functional Materials

We have proposed three relationships for reversibility: $\det \mathbf{U}_1 = 1$ (and, as many compatible variants of martensite as possible), $\lambda_2 = 1$, λ_2 being the middle eigenvalue of $\mathbf{U}_1$, and the cofactor conditions

$$\lambda_2 = 1, \quad \operatorname{tr} \mathbf{U}_1^2 - \det \mathbf{U}_1^2 - 2 - \frac{1}{4}|\mathbf{a}|^2 > 0, \quad \mathbf{a} \cdot \mathbf{U}_1 \operatorname{cof} (\mathbf{U}_1^2 - \mathbf{I})\mathbf{n} = 0\,. \quad (9.10)$$

The experimental evidence rather strongly suggests that the first two of these govern the main part of the hysteresis, while the third condition is a natural extension of these concepts. The standard ideas that are usually quoted as governing hysteresis in martensitic phase transitions do not seem to us to be the most influential factors.

More generally, our idea can be expressed as follows. *Arrange to have a big first order, reversible (martensitic, i.e., diffusionless) phase transformation that separates two phases with different electromagnetic properties.* This leads to the following advantageous situation. (1) Since the two phases have different lattice parameters, and different band structures, the possibilities for simultaneous unlikely properties are greatly improved. (2) If the phase transformation is reversible then the volume fraction of the two phases could be changed by using an electric field, a magnetic field, or a stress, depending on the shape change and electromagnetic properties of the two phases.

Besides ferroelectricity – ferromagnetism, there are many potential property pairs that exhibit lattice parameter sensitivity and are candidates for the proposed strategy: solubility–insolubility of H_2, high band gap–low band gap semiconductors, insulator–conductor (electrical or thermal), opaque–transparent (at various wavelengths), high–low index of refraction, luminescent–nonluminescent. Also possible according to this strategy are new kinds of thermoelectric and thermomagnetic materials, that utilize the lattice parameter sensitivity of electromagnetic properties together with the latent heat of transformation.

Acknowledgments

We are grateful to K. Rabe, M. Wuttig, E. Quandt, J.M. Ball, T. Shield, J. Cui and B. Berg for stimulating discussion of these ideas. This work was supported by MURI N00014-010100761 administered by ONR. The work also benefitted from the support of NSF-NIRT DMS-0304326.

References

1. N.A. Hill: J. Phys. Chem. B **104**, 6694 (2000)
2. N.A. Hill: Annu. Rev. Mater. **32**, 1 (2002)

3. N. Hill, K.M. Rabe: Phys. Rev. B **53**, 8759 (1999)
4. R.E. Cohen: J. Phys. Chem. Solids **61**, 139 (1999)
5. Y.C. Yang, X.D. Zhang, S.L. Ge, Q. Pan, L.S. Kong, H. Li, J.L. Yang, B.S. Zhang, Y.F. Ding, C.T. Ye: J. Appl. Phys. **70**, 6001 (1991)
6. J. Wang, J.B. Neaton, H. Zheng, V. Nagarajan, S.B. Ogale, B. Liu, D. Viehland, V. Vaithyanathan, D.G. Schlom, U.V. Waghmare, N.A. Spaldin, K.M. Rabe, M. Wuttig, R. Ramesh: Science **299**, 1719 (2003)
7. R. Tickle, R.D. James: J. Magn. Magn. Mater. **195**, 627 (1999)
8. H.A. Jahn, E. Teller: Proc. R. Soc. London **A161**, 220 (1937)
9. R.M. Tabanli, N.K. Simha, B.T. Berg: Metall. Mater. Trans. A **32**, 1866 (2001); Mater. Sci. Eng. A, **273**, 644 (1999)
10. K. Otsuka, H. Sakamoto, K. Shimizu: Acta Metall. **27**, 585 (1979)
11. S. Miyazaki, K. Otsuka: ISIJ Int. **29**, 353 (1989)
12. R.D. James, K. Hane: Acta Mater. **48**, 197 (2000)
13. K. Bhattacharya: Arch. Rational Mech. Anal. **120**, 201 (1992)
14. J.M. Ball, R.D. James: Arch. Rational Mech. Anal. **100**, 13 (1987)
15. J.M. Ball, R.D. James: Philos. Trans. R. Soc. London **A338**, 389 (1992)
16. R.V. Kohn, S. Müller: Philos. Mag. A **66**, 697 (1992); Commun. Pure Appl. Math. **47**, 405 (1994)
17. Z. Zhang: MS thesis, University of Minnesota (2004)
18. B. Winzek, E. Quandt: Proc. Mater. Res. Soc. Symp. **604**, 117 (2000)